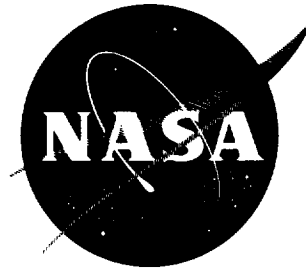


N62-71605

NASA TN D-1031

NASA TN D-1031



TECHNICAL NOTE

D-1031

RADIATION EMISSION EFFECTS OF THE EQUILIBRIUM BOUNDARY
LAYER IN THE STAGNATION REGION

By John Thomas Howe

Ames Research Center
Moffett Field, Calif.

NATIONAL AERONAUTICS AND SPACE ADMINISTRATION
WASHINGTON

September 1961

NATIONAL AERONAUTICS AND SPACE ADMINISTRATION

TECHNICAL NOTE D-1031

RADIATION EMISSION EFFECTS OF THE EQUILIBRIUM BOUNDARY
LAYER IN THE STAGNATION REGION

By John Thomas Howe

SUMMARY

The laminar compressible boundary layer in chemical equilibrium is analysed to show the effect of emission of radiation by the boundary layer on solutions of the energy equation and on the resulting heat transfer. Solutions are obtained at one flight condition, but for several nose radii, in a regime where absorption is negligible. The consequent effects on heat transfer and boundary-layer thickness are determined. The concept of a separate boundary layer and shock layer is discussed in the light of the results obtained.

INTRODUCTION

The advent of atmospheric flight at speeds greater than circular satellite speed has introduced a number of problems associated with the very high temperatures that exist in the air behind the bow shock wave of a bluff body. One of these problems concerns the effects of the emission of thermal radiation from the chemically dissociated air at these high temperatures. From the results of shock tube experiments and theory, Kivel and Bailey (ref. 1) have made predictions of the emission of radiant energy from high-temperature air in equilibrium. Kivel (ref. 2) has applied these results to study stagnation heating by radiation emitted from the inviscid isothermal shock layer.

The Kivel study is a first look at the problem and, of course, ignores the effects of gaseous radiation on the structure of the shock layer. In Kivel's work and in other studies of shock layer gaseous radiation, the radiation from the boundary layer is generally assumed implicitly to be negligible and there is assumed to be no boundary-layer interaction with the shock layer.

Smith (ref. 3) in an early analysis, performed from the boundary-layer point of view, estimated radiation effects in the boundary layer by studying the energy equation in which the convective terms were neglected. The results of a numerical example in which water vapor

emissivities were used and temperature profiles were assumed to be unaffected by radiation indicated that radiation emitted by the boundary layer has negligible effects on boundary-layer behavior.

More recently, the problem has been formulated quite elegantly by Goulard (ref. 4) and again by Tellep and Edwards (ref. 5).. They treat the radiation boundary-layer problem in the exact sense by combining the astrophysic radiative transfer theory with boundary-layer theory. There is some difficulty inherent in solving the resulting set of equations, one of which is an integrodifferential equation. No solutions were attempted in reference 5. To solve the equations in the stagnation region, it is necessary to evaluate the integral part of the integrodifferential equation over the shock layer. Thus a detailed knowledge of the radiating shock layer is essential to solving the boundary layer. For this reason, the practicality of trying to solve these equations in the stagnation region boundary layer is questionable.

The purpose of the present paper is to study the radiation problem from the boundary-layer point of view, using some approximations that make the problem simpler than outlined by reference 5, and yet to use recent information concerning the emission properties of air. The aim will be to verify that there is negligible boundary-layer radiation, that temperature profiles are unaltered, that conduction at the wall is unaltered, and that wall effects are not felt far from the wall - in short, that the shock-layer approach to the radiation problem which ignores a boundary-layer effect is satisfactory. In analysing the radiating boundary-layer problem, the usual boundary-layer assumptions will be made. The results should either provide the verification sought or lead to a result that contradicts some of the boundary-layer concepts. Hopefully, in the event that the contradiction occurs, the results would at least suggest a further approach to the problem.

In this analysis the simplification concerning the radiation effect arises if the gas emits but does not absorb radiation to any extent. Then the equations to be solved are differential equations instead of integrodifferential equations. Thus we set out to solve the boundary-layer problem in which there is emission of radiation but no reabsorption. Fortunately, this is a very reasonable assumption for some interesting flight conditions. An unpublished study by K. K. Yoshikawa of Ames Research Center concerning the emission and absorption of radiation in the equilibrium shock layer shows that in a broad flight regime, the radiant energy absorbed is negligible compared with that emitted. This situation is attributable to the fact that the amount of energy absorbed depends, in part, on the radiation path length, and for a broad flight regime, the path lengths are too short for appreciable absorption. The no-absorption regime corresponds roughly to flight at speeds less than escape speed at altitudes above 150,000 feet for bodies having a shock standoff distance of less than 1 foot. In the present analysis examples will be studied in the flight regime where absorption in the shock layer is negligible and it will be assumed that absorption in the boundary-layer air is also negligible.

In addition to the above assumption, it is assumed that the boundary layer is in chemical equilibrium, that Prandtl number is constant, and that Lewis number is unity. Finally, it is assumed that the only non-adiabatic effect in the inviscid shock layer is the emission of radiation. Although the analysis is formulated for either two-dimensional or axisymmetric flow, the examples computed will be for axisymmetric flow only and will pertain to bodies of different nose radii flying at 31,000 feet per second at an altitude of 165,000 feet. For this flight condition, it is noted that figure 4 of reference 6 shows the assumption of equilibrium flow in the boundary layer is valid.

SYMBOLS

a	exponent in equation (A5)
C	Chapman-Rubesin function (eq. (19))
c	coefficient in radiation emission equation (A5)
c_{p_i}	specific heat of species i
\bar{c}_p	frozen specific heat $\sum c_i c_{p_i}$
c_i	mass fraction of species i
d	exponent in radiation emission equation (A5)
D	coefficient of self diffusion
E_t	the rate of total radiant energy emission per unit volume of gas
f	dimensionless stream function (eq. (21))
F	dimensionless stream function (eq. (47))
\vec{F}	radiation flux
g	ratio of total enthalpy to total enthalpy at the edge of the boundary layer, $\frac{j}{j_e}$
h	static enthalpy
h_i^0	heat of formation of i th species at 0°K
j	total enthalpy
k	thermal conductivity

K	function defined by equation (30)
K_0	function K evaluated at 7500° K
l_D	heat of dissociation
Le	Lewis number, $\frac{\bar{c}_p \rho D}{k}$
M	molecular weight of species
m	exponent in equation (1); zero for two-dimensional flow, unity for axisymmetric flow
n	exponent in equation (A5)
p	pressure
\overline{Pr}	Prandtl number, $\frac{\bar{c}_p \mu}{k}$
q	heat-transfer rate or energy
r_0	radius of cross section of body
R	universal gas constant or body nose radius
s	dimensionless coordinate parallel to body surface, equation (15)
t	time
T	temperature
T_0	reference temperature (7500° K)
u	velocity parallel to body surface
v	velocity normal to body surface
w_i	mass rate of production of species i per unit volume
x	coordinate parallel to body surface
y	coordinate normal to body surface
α	intercept in equation (A1)
β	velocity gradient at stagnation point (eq. (24))
δ	thermal boundary-layer thickness
η	dimensionless coordinate normal to body surface (eq. (16))

μ	coefficient of viscosity
ρ	gas density
ρ_0	reference density (sea level air density)
τ	slope in equation (A1)
ψ	stream function
ξ	$\frac{\eta}{\sqrt{2}}$

Superscripts

$',",'''$	derivatives with respect to the independent variable concerned
-----------	--

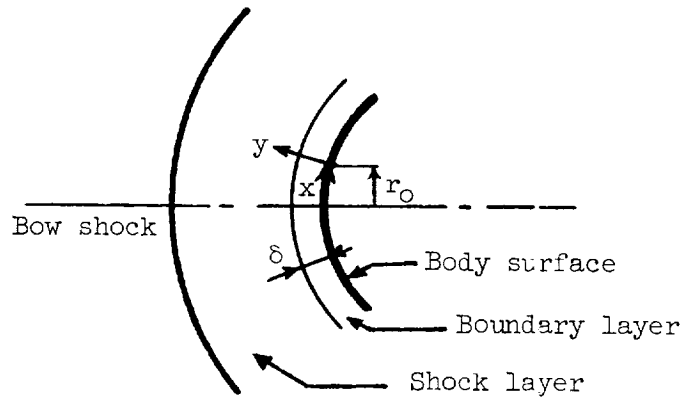
Subscripts

e	outer edge of the boundary layer
i	species i
o	reference conditions
r	radiant
s	stagnation
∞	conditions in undisturbed stream
1	atoms
2	molecules

ANALYSIS

Basic Differential Equations

The physical model chosen for analysis is shown in sketch (a). As usual, the region between the bow shock and the body is divided into an inviscid shock layer and a boundary layer, both of which emit radiation.



Sketch (a)

The boundary-layer equations expressing continuity of mass, the momentum theorem, conservation of energy, and concentration of species for a chemically reacting gas are, respectively,

$$\frac{\partial}{\partial x} (\rho u r_0^m) + \frac{\partial}{\partial y} (\rho v r_0^m) = 0 \quad (1)$$

$$\rho u \frac{\partial u}{\partial x} + \rho v \frac{\partial u}{\partial y} = - \frac{dp}{dx} + \frac{\partial}{\partial y} \left(\mu \frac{\partial u}{\partial y} \right) \quad (2)$$

$$\begin{aligned} \rho u \frac{\partial j}{\partial x} + \rho v \frac{\partial j}{\partial y} &= \frac{\partial}{\partial y} \left(\frac{\mu}{Pr} \frac{\partial j}{\partial y} \right) + \frac{\partial}{\partial y} \left[\mu \left(1 + \frac{1}{Pr} \right) \frac{\partial}{\partial y} \left(\frac{u^2}{2} \right) \right] \\ &+ \frac{\partial}{\partial y} \left[\rho D \left(1 - \frac{1}{Le} \right) \sum h_i \frac{\partial c_i}{\partial y} \right] - \text{div } \vec{F} \end{aligned} \quad (3)$$

and

$$\rho u \frac{\partial c_i}{\partial x} + \rho v \frac{\partial c_i}{\partial y} - \frac{\partial}{\partial y} \left(\rho D \frac{\partial c_i}{\partial y} \right) = w_i \quad (4)$$

Note that since the boundary layer is assumed to be in chemical equilibrium, equation (4) will not be used to determine the degree of dissociation; it can be computed directly from local properties. In addition, the equation of state of the gas is

$$p = \rho \frac{R}{M} T \quad (5)$$

where

$$M = \left(\sum \frac{c_i}{M_i} \right)^{-1} \quad (6)$$

and the definition of total enthalpy is

$$j = h + \frac{u^2}{2} = \sum c_i h_i + \frac{u^2}{2} \quad (7)$$

where

$$h_i = \int_0^T c_{p_i} dT + h_i^0 \quad (8)$$

The exponent m in equation (1) is zero for two-dimensional flow and unity for axisymmetric flow. The third term on the right of equation (3) is zero because Le is assumed to be unity. The last term in equation (3), $\text{div } \vec{F}$, represents the rate at which energy is emitted by the unit gas volume minus the rate at which energy is absorbed by the unit gas volume. It was explained previously that we will be concerned with the flight regime in which absorption is negligible compared with emission. Then the $\text{div } \vec{F}$ in equation (3) is simply the rate at which energy is emitted per unit volume of gas.

The Radiation Term

As previously mentioned, reference 1 presents predictions of the rate of radiant energy emission per unit volume of equilibrium air as a function of temperature and density. In appendix A of the present paper, the results of reference 1 are correlated empirically (eq. (A5)) such that the total rate of energy emission per unit volume (which is now equated to $\text{div } \vec{F}$) is given by the expression

$$\text{div } \vec{F} = E_t = cT^d \left(\frac{\rho}{\rho_0} \right)^{nT^a} \quad (9)$$

where c , d , n , and a are constants appropriately chosen for the regime of interest.

Boundary Conditions

The boundary conditions for equations (1) through (3) are at $y = 0$;

$$u = 0, v = 0, j = j_w \quad (10)$$

as $y \rightarrow \infty$,

$$u \rightarrow u_e \quad (11)$$

Another boundary condition on y is obviously required. For solutions of the boundary-layer energy equation without radiation, it is usually specified that j approach j_e asymptotically as y approaches ∞ , which implies that both the first and second derivatives of j with respect to y approach zero at the outer edge of the boundary layer. This, of course, is compatible with the usual shock-layer energy equation (for an inviscid nonconducting gas without radiation) which is

$$\rho \frac{Dj}{Dt} = 0 \quad (12)$$

Thus j is constant and there are no gradients of j in the shock layer at the outer edge of the boundary layer.

Now that we have radiation emission from the shock layer and the boundary layer, it is necessary to provide a new boundary condition compatible with the radiating shock and boundary layer. Since the shock layer is emitting radiation, we must modify the right-hand side of the energy equation (12). If the emission of radiation is assumed to be the only nonadiabatic effect in the shock layer, the modified energy equation is

$$\rho \frac{Dj}{Dt} = -\text{div } \vec{F} \quad (13)$$

or if the Eulerian derivative is written for the steady state, and the boundary-layer coordinate system is assumed to be valid in the shock layer near the boundary layer,

$$\rho u \frac{\partial j}{\partial x} + \rho v \frac{\partial j}{\partial y} = -\text{div } \vec{F} \quad (14)$$

Subsequently, equation (14) will be transformed in the same way the boundary-layer equations are transformed and will be used to provide the second boundary condition required.

Transformations

Equations (1), (2), and (3) and their boundary conditions (10) and (11) are to be transformed from x and y as independent variables to s and η by means of the Levy transformation (ref. 7), a stream function, several definitions and assumptions, and some exterior flow relationships as follows:

The Levy transformation is

$$s = \int_0^x \rho_e u_e \mu_e r_o^{2m} dx \quad (15)$$

$$\eta = \frac{u_e r_o^m}{\sqrt{2sC}} \int_0^y \rho dy \quad (16)$$

A stream function is defined so that

$$\frac{\partial \psi}{\partial y} = \rho u r_o^m, \quad - \frac{\partial \psi}{\partial x} = \rho v r_o^m \quad (17)$$

and the continuity equation (1) is satisfied. The following quantities are defined

$$g(\eta) = \frac{j}{j_e} \quad (18)$$

$$\frac{\rho \mu}{\rho_e \mu_e} = C \quad (19)$$

(where C , the Chapman-Rubesin function of reference 8 is assumed constant) and

$$f'(\eta) = \frac{u}{u_e} \quad (20)$$

from which

$$f(\eta) = \frac{\psi}{\sqrt{2sC}} \quad (21)$$

In the bluff body stagnation region it is assumed that

$$r_o = x \quad (22)$$

At the outer edge of the boundary layer, the external velocity is described by

$$u_e = \beta x \quad (23)$$

where from modified Newtonian flow concepts in the stagnation region

$$\beta = \frac{1}{R} \sqrt{\frac{2(p_s - p_\infty)}{(\rho_e)_s}} \quad (24)$$

It is further assumed that

$$\rho_e \mu_e = (\rho_e \mu_e)_s \quad (25)$$

Use of equations (22), (23), and (25) in equations (15) and (16) yields

$$s = \frac{\beta \rho_e \mu_e x^{2(m+1)}}{2(m+1)} \quad (26)$$

$$\eta = \sqrt{\frac{(m+1)\beta}{c \rho_e \mu_e}} \int_0^y \rho \, dy \quad (27)$$

Thus, s is proportional to x^2 and x^4 for two-dimensional and axisymmetric flows, respectively, while η is a function of y weighted by the density variation.

Transformation of equations (2) and (3) to the new independent variables s and η by means of the defined quantities and assumptions results in the following set of ordinary differential equations (for constant \overline{Pr})

$$f'''' + ff'' = \frac{2s}{u_e} \frac{du_e}{ds} \left(f'^2 - \frac{\rho_e}{\rho} \right) \quad (28)$$

$$\frac{g''}{\overline{Pr}} + fg' - \left[\frac{cT^d \left(\frac{\rho}{\rho_0} \right)^{nT^a}}{(m+1)\beta j_e \rho} \right] = - \frac{u_e^2}{j_e} \frac{\partial}{\partial \eta} \left[\left(1 - \frac{1}{\overline{Pr}} \right) f' f'' \right] \quad (29)$$

The right-hand side of equation (28) will be neglected by virtue of the qualitative physical argument of reference 9 (based on the fact that the

surface temperature is much lower than T_e). The right-hand side of equation (29) will be neglected because $u_e^2 \ll j_e$ in the stagnation region in hypersonic flow. Thus if T and ρ in equation (29) are expressed in terms of $g(\eta)$, similarity solutions of both equations (28) and (29) can be obtained. This is done by representing the chemically reacting air as a binary mixture of air atoms and air molecules in equilibrium. Now letting subscript 1 denote atoms and subscript 2 denote molecules, we write the law of mass action in terms of the partial pressures (ref. 10, p. 28)

$$p_1^2 p_2^{-1} = K(T) \quad (30)$$

Using the species equation of state

$$p_i = c_i \frac{R}{M_i} \rho T \quad (31)$$

and the fact that

$$M_2 = 2M_1 \quad (32)$$

in equation (30) yields

$$\frac{4c_1^2 p}{1 - c_1^2} = K(T) \quad (33)$$

Also from reference 10 (p. 30)

$$\frac{d(\ln K)}{dT} = \frac{M_2 l_D}{RT^2} \quad (34)$$

The heat of dissociation (noting that the heat of formation of the air molecule is zero)

$$l_D = h_1^0 - h_2^0 = h_1^0 \quad (35)$$

is assumed constant. Integrating equation (34) and substituting the result in equation (33) with the boundary conditions $K = K_0$ at $T = T_0$ yields

$$K(T) = K_0 e^{\frac{M_2 l_D}{R} \left(\frac{1}{T_0} - \frac{1}{T} \right)} = \frac{4c_1^2 p}{1 - c_1^2} \quad (36)$$

Reference 11 shows that when a mixture of air atoms and air molecules is assumed, c_{p1} and c_{p2} are both almost constant in a temperature range

from 2,000° to 9,000° K, and they differ from one another by less than 15 percent. Thus we will arbitrarily choose a constant common value of $c_{p1} \approx c_{p2} \approx 0.318$ Btu/lb °R between them such that any deviation from that common value is less than 10 percent. Then from equation (7) using equation (18) and the fact that $u^2 \ll 2j_e$ in the stagnation region

$$\frac{j}{j_e} = \frac{c_{p2} T + c_1 l_D}{j_e} = g(\eta) \quad (37)$$

or

$$T = \frac{j_e g(\eta) - c_1 l_D}{c_{p2}} \quad (38)$$

Eliminating c_1 between equations (36) and (38) yields

$$T = \frac{1}{c_{p2}} \left[j_e g(\eta) - l_D \sqrt{\frac{1}{1 + \frac{4p}{K_0} e^{-\frac{M_2^2 D}{F} \left(\frac{1}{T_0} - \frac{1}{T} \right)}}} \right] \quad (39)$$

Now T is a function of g (or η) alone (if we consider that p is essentially constant in the stagnation region). By use of equations (5), (6), and (38), ρ becomes a function of T and hence, η

$$\rho = \frac{M_2 p l_D}{(l_D + j_e g - c_{p2} T) R T} \quad (40)$$

If equation (40) is used in equation (29), and the right-hand sides of equations (28) and (29) are omitted, the differential equations become

$$f''' + f f'' = 0 \quad (41)$$

$$\frac{g''}{Pr} + f g' - \left[\frac{c T^d}{(m+1) \beta j_e \rho_0} \right] \left[\frac{M_2 p l_D}{\rho_0 R T (l_D + j_e g - c_{p2} T)} \right]^{n T^a - 1} = 0 \quad (42)$$

where T is given by equation (39). The boundary conditions become (from eqs. (10) and (11)) at $\eta = 0$,

$$f = f' = 0, \quad g = g_w \quad (43)$$

at $\eta \rightarrow \infty$,

$$f' \rightarrow 1 \quad (44)$$

The outer boundary condition on equation (42) is developed by use of equation (14) for the shock layer. Transformation of equation (14) in the same manner as equations (1), (2), and (3) yields the energy equation for the shock layer adjacent to the boundary layer

$$fg' = \left[\frac{cT^d}{(m+1)\beta j_e \rho_o} \right] \left[\frac{M_2 p l_D}{RT \rho_o (l_D + j_e g - c_{p2} T)} \right]^{nT^a-1} \quad (45)$$

Equation (45) is an expression for the first derivative of g . Applying equations (42) and (45) at the edge of the boundary layer (at $g = 1$) shows that

$$g_e'' = 0 \quad (46)$$

Of course, precisely the same result could have been derived if conduction and diffusion effects had been required to vanish at the edge of the boundary layer. Equation (41) is the Blasius equation of reference 12 if η is related to the Blasius ξ and $f(\eta)$ and its derivations are related to the Blasius $F(\xi)$ and its derivatives by

$$\left. \begin{aligned} \eta &= \sqrt{2} \xi \\ f(\eta) &= F(\xi)/\sqrt{2} \\ f'(\eta) &= F'(\xi)/2 \\ f''(\eta) &= F''(\xi)/2\sqrt{2} \end{aligned} \right\} \quad (47)$$

Equations (47) cause the boundary conditions on $f(\eta)$ to be compatible with those on $F(\xi)$ in reference 12. Thus the solution of equation (41) can be obtained from reference 12. It is noted that although a similarity type solution of equation (42) is possible, generality is lost in that it is necessary to specify a nose radius (for β) and flight condition for each solution.

Heat Transfer to the Wall

From the solutions of the energy equation, we want to determine the heat flux at the wall due to conduction and diffusion and, in addition, to determine how much radiant energy originating in the boundary layer

strikes the wall (radiant heat transfer to the wall from the region between the edge of the boundary layer and the shock is not included in this discussion). To evaluate the radiant energy, we simply assume that half the radiant energy emitted from each volume element in the boundary layer is directed toward the wall and half toward the shock layer. Then in the stagnation region the heat flux at the wall due to conduction, diffusion, and radiation emitted from the boundary layer is (for a nonreflecting wall)

$$q_w = - \left(k \frac{\partial T}{\partial y} - \rho D \sum_i h_i \frac{\partial c_i}{\partial y} \right)_w - \frac{1}{2} \int_0^\delta c T^d \left(\frac{\rho}{\rho_0} \right)^{n T^a} dy \quad (48)$$

or if equation (48) is rewritten and it is assumed that Le is unity

$$q_w = - \left(\frac{k}{c_p} \frac{\partial j}{\partial y} \right)_w - \frac{1}{2} \int_0^\delta c T^d \left(\frac{\rho}{\rho_0} \right)^{n T^a} dy \quad (49)$$

Transforming equation (49) as before and making use of equation (27) yields

$$q_w = - \frac{j_e g_w'}{\overline{Pr}} \sqrt{(m+1) C \rho_e \mu_e \beta} - \frac{c}{2 \rho_0} \sqrt{\frac{C \rho_e \mu_e}{\beta(m+1)}} \int_0^{\eta_e} T^d \left[\frac{v_2 p l_D}{(l_D + j_{e3} - c_{p2} T) R \rho_0 T} \right]^{n T^a - 1} d\eta \quad (50)$$

The first term is thus the combined conduction and diffusion heat flux and the second term is the radiative heat transfer from boundary-layer air for a nonreflecting wall (hereafter referred to as q_{re}).

Numerical Solution

Equations (41) and (42) were solved simultaneously subject to boundary conditions (43), (44), and (46). The solutions were obtained using the Adams Moulton (ref. 13, p. 200) predictor corrector numerical integration method programmed for the IBM 704 electronic data processing machine. The value of g_w' needed to start the numerical solution of equation (42) was determined by trial and error so that the boundary condition (46) was satisfied. The specified value of g_w corresponds to the wall temperature cited below. All examples corresponded to flight

of axisymmetric bodies of varying nose radii at a speed of 31,000 feet per second at an altitude of 165,000 feet. The wall temperature was fixed at 2000° K. Values of l_D and K_0 were obtained by matching equations (36) and (37) with results of reference 14 at a reference temperature of 7500° K.

It became increasingly difficult to obtain solutions as the body nose radius increased. The boundary layer thickened, accuracy demanded smaller integration steps, and matching boundary conditions became more difficult. Solutions were obtained, however, for body nose radii up to 10 feet.

DISCUSSION OF THE RESULTS

In the analysis of this problem, several simplifying assumptions have been made. Also, the equation by which the radiation emission is calculated is an approximation to experimental results. For these reasons, the results of the analysis are not considered to be exact, but are intended to show qualitative effects.

We will examine in some detail the influence of the radiation term on the solution of the energy equation. Furthermore, the influence of the radiation term on both convective and total heat transfer will be evaluated.

Solutions of the energy equation in terms of total enthalpy are shown in figure 1. The upper curve is the enthalpy profile for bodies of all radii if there is no radiation term in the energy equation. The lower curve corresponds to a solution with radiation emission and pertains to a body with a nose radius of 10 feet. Curves of radiation emission for smaller nose radii lie between those shown. It is important to note that the curve for the no-radiation case goes to unity fairly rapidly, while the curve with radiation approaches unity very slowly (at values of η greater than those shown). The emission of radiation effectively thickens the thermal boundary layer (thickness here being defined by that point where equation (47) is satisfied) thus including more of the shock layer air within the boundary layer.

The temperature profiles corresponding to the enthalpy profiles are shown in figure 2. Again, the upper curve corresponds to the usual solution of equation (43) for all body sizes if the radiation term is omitted. It exhibits the usual inflections for equilibrium boundary layers (these inflections are also evident in similar plots presented in ref. 15). Again, the upper curve for the no-radiation case converges to unity very rapidly. The lower curves in figure 2 correspond to solutions of equation (43) with the radiation term included and are for nose radii of 3 and 10 feet. Here the difference between the radiation and no-radiation solutions is somewhat more pronounced than the differences

observable on the previous figure. The thermal boundary layer is thicker and, of course, conduction and diffusion effects are felt much farther from the wall.

It should also be noted that the emission of radiation by the boundary layer diminishes the temperature and enthalpy gradients at the wall small amounts (actually somewhat too small to be seen on fig. 2). Such a result is to be expected since the greater proportion of radiation is emitted from the hotter air not in close proximity to the wall. It can be anticipated that the corresponding reduction in convective heat transfer is more than offset by the added radiant heating load. More will be said of this in connection with a subsequent figure.

Figure 3 shows the distribution of radiant energy emitted in the boundary layer normalized to the value at the edge of the boundary layer for the nose radii of 3, 5, and 10 feet. The figure shows that the emission rate rises rapidly up to $\eta \approx 5$, after which it rises more gradually to unity at the boundary-layer edge. If η were linearly related to y , the area under a given curve up to any value of η would be proportional to $q_r(\eta)$, the rate of total radiant energy emission from the layer of air between the wall and η . However, because of the compressibility effect, η is not linearly related to y (see eqs. (16) and (27)), and to obtain $q_r(\eta)$ as a function of η , it is necessary to perform the integration shown in equation (51), where $q_r(\eta)/q_{re}$ is the ratio of the radiant energy emitted from the layer of air between the wall and η to the total radiant energy emitted by the boundary layer:

$$\frac{q_r(\eta)}{q_{re}} = \frac{\int_0^\eta T^d \left[\frac{M_2 p l_D}{(\lambda_D + j_{eg} - c_{p_2} T) \rho_2 RT} \right]^{nT^a-1} d\eta}{\int_0^{\eta_e} T^d \left[\frac{M_2 p l_D}{(\lambda_D + j_{eg} - c_{p_2} T) \rho_2 RT} \right]^{nT^a-1} d\eta} \quad (51)$$

The ratio is plotted in figure 4. Without the radiation term in the energy equation, the solution converged at a value of η of roughly 10 for all nose radii. Thus the figure shows that most of the radiation emitted by the boundary layer is from air that for the no-radiation case would have been outside the boundary layer.

The ratio of the total heating load (computed from eq. (51)) including incident radiation from the boundary layer to heat transfer without radiation is plotted as a function of nose radius in figure 5. It should be noted that the comparison does not include the radiation contribution from the region between the edge of the boundary layer and the shock wave.

It was mentioned previously that the slight reduction of convective heating due to boundary-layer radiation emission is more than offset by the added radiative heating. This is shown in the figure by the fact that the ratio plotted is always greater than unity. For the 3-foot nose radius, the total heat transfer is increased by almost one third because of radiation heating, and for the 10-foot nose radius, it is more than doubled.

A
5
0
9
Now that the detailed solutions of the boundary-layer energy equation in the no-absorption regime have been discussed, it is pertinent that an evaluation be made of the boundary-layer approach for studying gas-dynamic effects in the stagnation region when self-radiation is important. In the analysis, several simplifying assumptions and concepts have been used. It is not usually possible to assess the full significance of all the assumptions in advance, but one hopes to be able to tell by the resulting solutions just how reasonable his assumptions were. In the present case, one further step has been made in the usual boundary-layer analysis in order to include the effect of radiation emission. In the resulting solutions the momentum boundary layer was unchanged. However, the solutions of the energy equation showed that its boundary conditions were satisfied at distances from the wall several times that of the corresponding no-radiation case. Indeed, the thermal boundary-layer thicknesses were comparable to the thicknesses usually calculated for the inviscid adiabatic shock layer. For this reason, the concept of a thermal boundary layer (to which conduction and diffusion effects are limited) separate and distinct from a shock layer loses its usefulness.

The results leading to this conclusion were obtained for the no-absorption case. An attempt was also made to solve the very strong absorption case. The results of that effort will not be discussed except to say that the remarks of the preceding paragraph also apply to the very strong absorption case, and additionally that the convective heating at the wall is greatly altered by radiation effects for the very strong absorption case.

The next approach to studying the gaseous radiation problem for the bluff body suggests itself. It is, of course, to solve the flow field from the wall to the shock including viscous, conduction, diffusion, and radiation effects in the flow equations. It is anticipated that such solutions would also give the shock standoff distance. Thus an attempt to obtain solutions from the body surface to the shock seems to be in order. In that light, the present study may be regarded as a first step toward this goal.

CONCLUDING REMARKS

The effects of radiation emission from the boundary-layer air have been studied by including an emission term in the energy equation. This

term was expressed by a relationship developed from experimental results of Kivel and Bailey. An appropriate boundary condition on the energy equation has been derived which limits conduction and diffusion effects to the boundary layer, and which allows the shock layer total enthalpy to vary as a result of the emission of radiation from the shock layer.

For the flight condition used in the solutions the emission of radiant energy diminishes the total enthalpy by a small amount. Similarly, the enthalpy gradient at the wall and thus the convective heat transfer are diminished slightly. However, the reduction in convective heat transfer is more than offset by an added radiant heat-transfer load.

Existence of an enthalpy gradient at the outer edge of the boundary layer and the self-emission of radiant energy increase the thickness of the thermal boundary layer by a large amount. More air (which is at an elevated temperature and is emitting radiation) is associated with the boundary layer. Conduction and diffusion effects are felt farther from the wall. For this reason, the concept of a thermal boundary layer separate and distinct from the shock layer when self-radiation is considered loses its usefulness in gaseous radiation studies that are more refined than those now in existence. At present the only way to calculate the gaseous radiation contribution to aerodynamic heating is to neglect the boundary layer and surface effects and use the shock layer results alone. Such an approach to estimating the radiative heat transfer, of course, gives no information of radiative effects on flow field structure, standoff distance or convective heating. Although the convective heating is not significantly affected in the present analysis for the no-absorption flight regime, it is greatly altered in the very strong absorption regime, and other methods must be used to study the problem. It is anticipated that in the intermediate regime (where self-absorption is significant but not excessive), convective heat transfer is substantially altered by the radiation effects, and that boundary layer and shock layer are again not separable. It is suggested that the next approach be to solve the flow field from the body to the shock without imposing a boundary-layer concept.

Ames Research Center
National Aeronautics and Space Administration
Moffett Field, Calif., June 20, 1961

APPENDIX A

CORRELATION OF RADIANT EMISSION DATA

Predictions of the total rate of radiant energy emission per unit volume from high-temperature air are given in reference 1. To utilize this information in the present analysis, it was necessary to derive an analytic expression for the variation of the radiant energy with temperature and density. Results from reference 1 are shown on figure 6 as dashed lines. Each curve (which was determined by five points) was replaced by its individual least squares best fit straight line. These are the straight lines shown in figure 6 and are represented by the expression

$$\log_{10} \left(\frac{E_t}{2} \right) = \log_{10} \alpha(T) + \tau(T) \log_{10} \left(\frac{\rho}{\rho_0} \right) \quad (A1)$$

or

$$\frac{E_t}{2} (\rho, T) = \alpha(T) \left(\frac{\rho}{\rho_0} \right)^{\tau(T)} \quad (A2)$$

where $\alpha(T)$ and $\tau(T)$ are listed on the figure. Secondly, all the slopes and all the intercepts $\log_{10} \tau(T)$ and $\log_{10} \alpha(T)$ were fitted by the least squares best fit straight line; that is, the lines

$$\log_{10} \tau(T) = \log_{10} n + a \log_{10} T \quad (A3)$$

and

$$\log_{10} \alpha(T) = \log_{10} \left(\frac{c}{2} \right) + d \log_{10} T \quad (A4)$$

were obtained. Combining equations (A2), (A3), and (A4) yields

$$E_t(\rho, T) = c T^d \left(\frac{\rho}{\rho_0} \right)^{n T^a} \quad (A5)$$

Thus all the lines in figure 7 were obtained from the single expression (A5) where c , d , n , and a are shown in the figure (where T is in $^{\circ}\text{K}$, and E_t is watts/cm³).

Although the representation of the prediction of reference 1 by equation (A5) is fair in figure 7, it can be improved in a restricted range of temperatures and densities if the technique is applied to the data of that range alone. The results of using the data in the temperature range 1000° to 8000° K and the density range $10^{-3} \leq \rho/\rho_0 \leq 10^{-1}$ are shown in figure 8. Equation (A5) with constants shown on figure 8 was used in the calculations of this paper.

REFERENCES

1. Kivel, B., and Bailey, K.: Tables of Radiation from High Temperature Air. Avco-Everett Res. Lab. Res. Rep. 21, Dec. 1957.
2. Kivel, Bennett: Radiation From Hot Air and Stagnation Heating. Avco-Everett Res. Lab. Res. Note 165, Oct. 1959.
3. Smith, John W.: Effect of Gas Radiation in the Boundary Layer on Aerodynamic Heat Transfer. Jour. Aero. Sci., vol. 20, no. 8, Aug. 1953, pp. 579-580.
4. Goulard, R., and Goulard, M.: Energy Transfer in a Couette Flow of a Radiant and Chemically Dissociating Gas. Preprints of papers of the 1959 Heat Transfer and Fluid Mechanics Inst., Stanford Univ. Press, 1959, pp. 126-139.
5. Tellep, D. M., and Edwards, D. K.: Paper II: Radiant-Energy Transfer in Gaseous Flows. Vol. I, Part One - Fluid Mechanics. General Research in Flight Sciences, Jan. 1959 - Jan. 1960. Lockheed Aircraft Corp., Missiles and Space Div., LMSD-288139, Jan. 1960.
6. Goodwin, Glen, and Chung, Paul M.: Effects of Nonequilibrium Flows on Aerodynamic Heating During Entry Into the Earth's Atmosphere From Parabolic Orbits. Proc. Second Int. Cong. for Aero. Sci., Zurich, Switzerland, Sept. 1960. Vol. 2, Advances in Aeronautical Sciences, Pergamon Press, N. Y., 1961.
7. Levy, Solomon: Effect of Large Temperature Changes (Including Viscous Heating) Upon Laminar Boundary Layers With Variable Free-Stream Velocity. Jour. Aero. Sci., vol. 21, no. 7, July 1954, pp. 459-474.
8. Chapman, Dean R., and Rubesin, Morris W.: Temperature and Velocity Profiles in the Compressible Laminar Boundary Layer With Arbitrary Distribution of Surface Temperature. Jour. Aero. Sci., vol. 16, no. 9, Sept. 1949, pp. 547-565. (Also IAS preprint 193, 1949.)
9. Lees, Lester: Laminar Heat Transfer Over Blunt-Nosed Bodies at Hypersonic Flight Speeds. Jet Propulsion, vol. 26, no. 4, April 1956, pp. 259-269, 274. (See also GALCIT Pub. 394.)
10. Liepmann, H. W., and Roshko, A.: Elements of Gas Dynamics. John Wiley and Sons, Inc., N. Y., 1957.

11. Scala, S. M., and Baulknight, C. W.: Transport and Thermodynamic Properties in a Hypersonic Laminar Boundary Layer, Part I - Properties of the Pure Species. ARS Jour., vol. 29, no. 1, Jan. 1959, pp. 39-45. (Also pub. as G. E. Doc. 58SD232 and G. E. Aerophysics Res. Memo 10, April 10, 1958.)
12. Emmons, H. W., and Leigh, D.: Tabulation of the Blasius Function With Blowing and Suction. (Combustion Aerodynamics Lab., Interim Tech. Dept. 9.) Harvard University, Div. of Applied Sciences, Nov. 1953.
13. Hildebrand, F. B.: Introduction to Numerical Analysis. McGraw-Hill Book Co., N. Y., 1956.
14. Moeckel, W. E., and Weston, Kenneth C.: Composition and Thermodynamic Properties of Air in Chemical Equilibrium. NACA TN 4265, 1958.
15. Fay, J. A., and Riddell, F. R.: Theory of Stagnation Point Heat Transfer in Dissociated Air. Jour. Aero Sci., vol. 25, no. 2, Feb. 1958, pp. 73-85, 121. (See also AVCO Res. Rep. 1.)

A
5
0
9

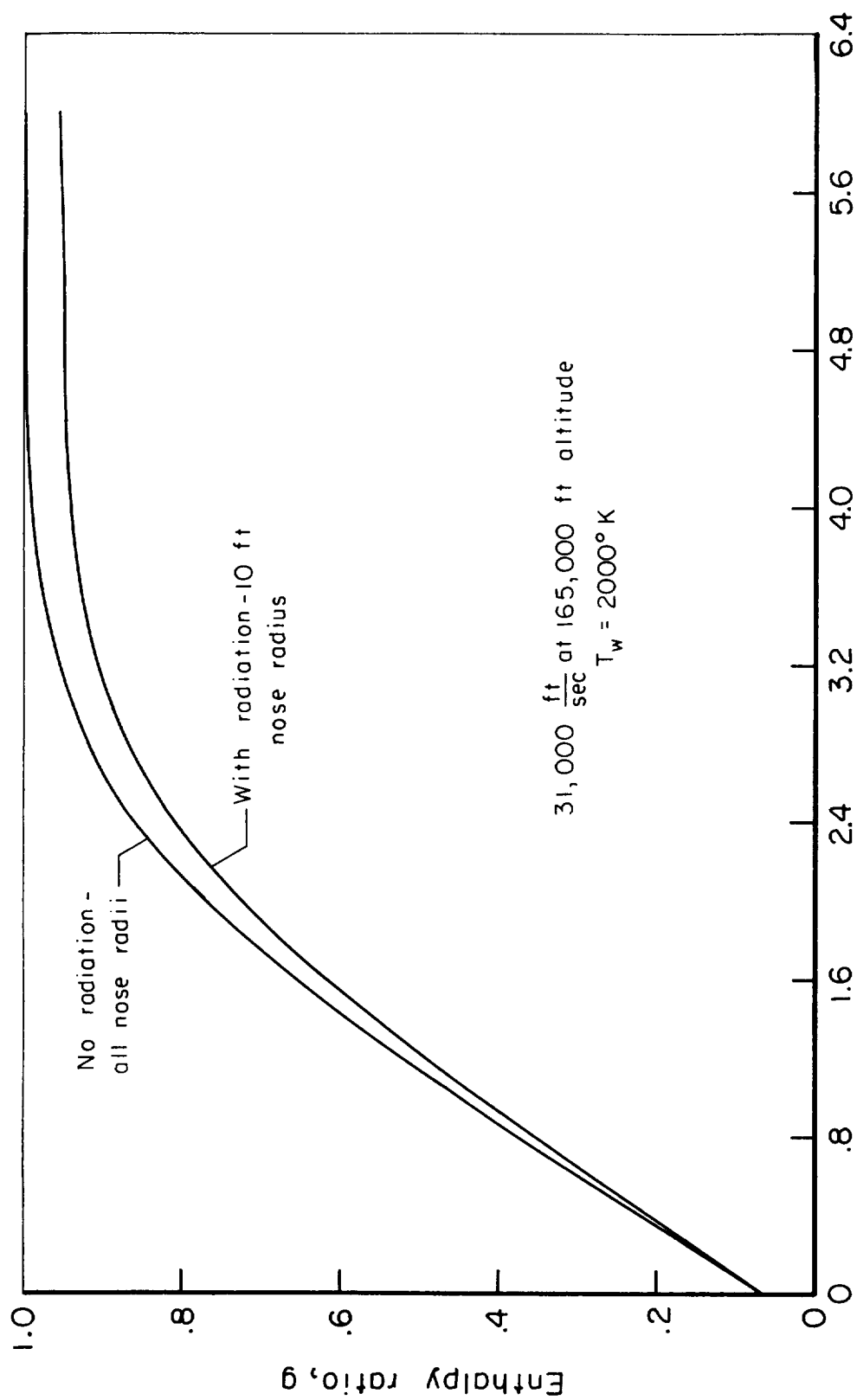


Figure 1.- Enthalpy profiles.

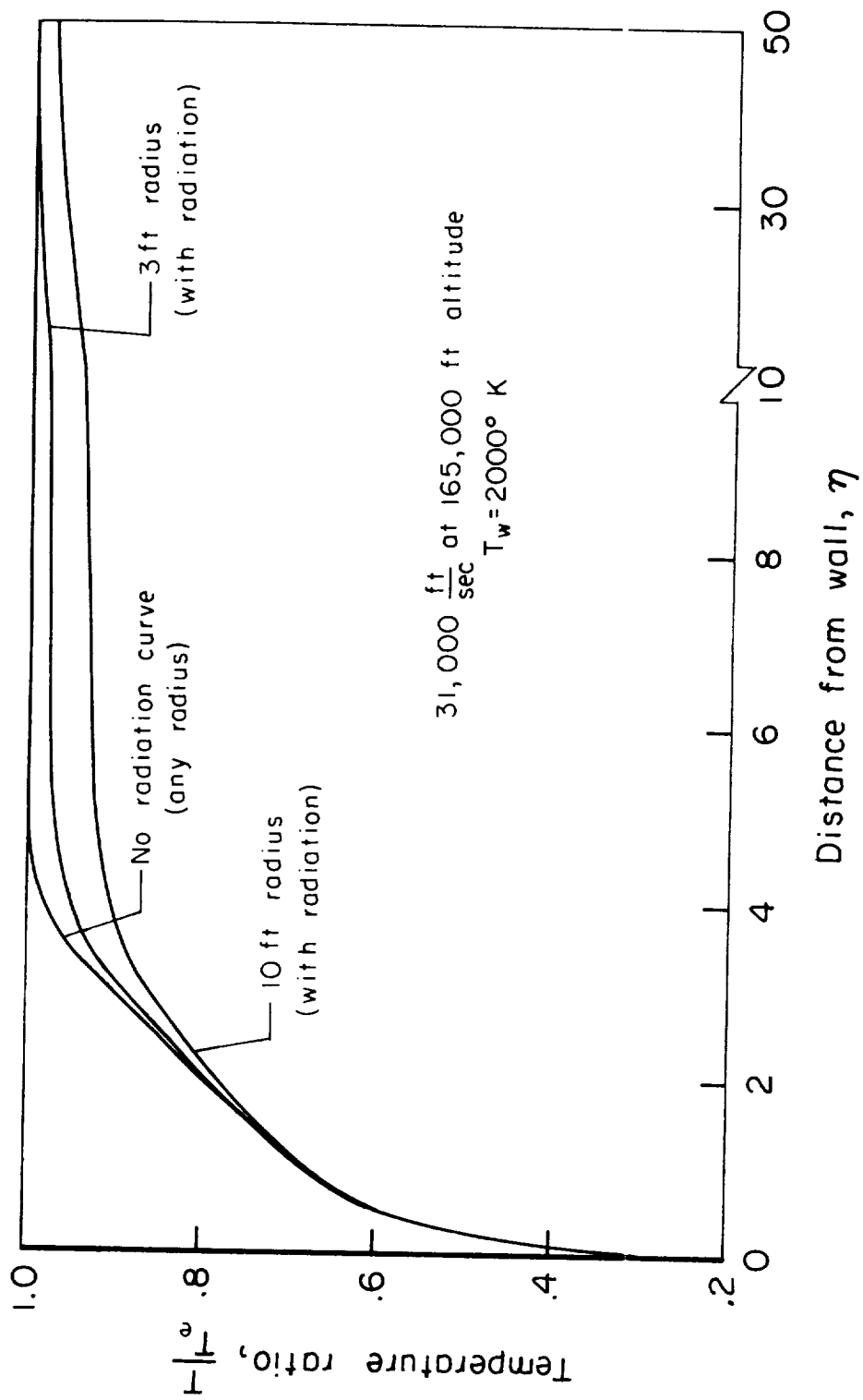


Figure 2.- Temperature profiles.

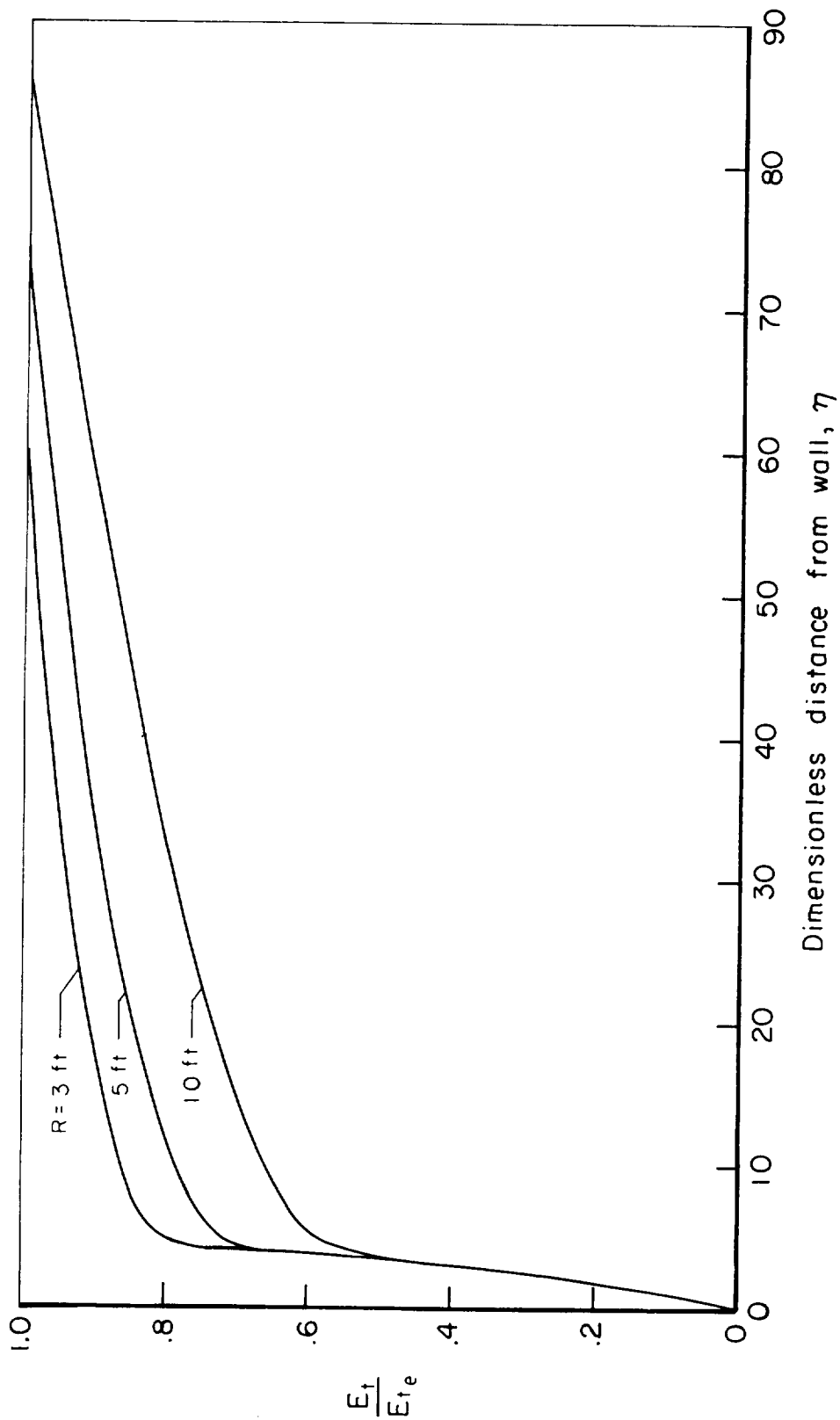


Figure 3.- Profiles of radiant energy distribution for various nose radii (31,000 ft/sec at 165,000 ft altitude, $T_w = 2000^\circ \text{ K}$).

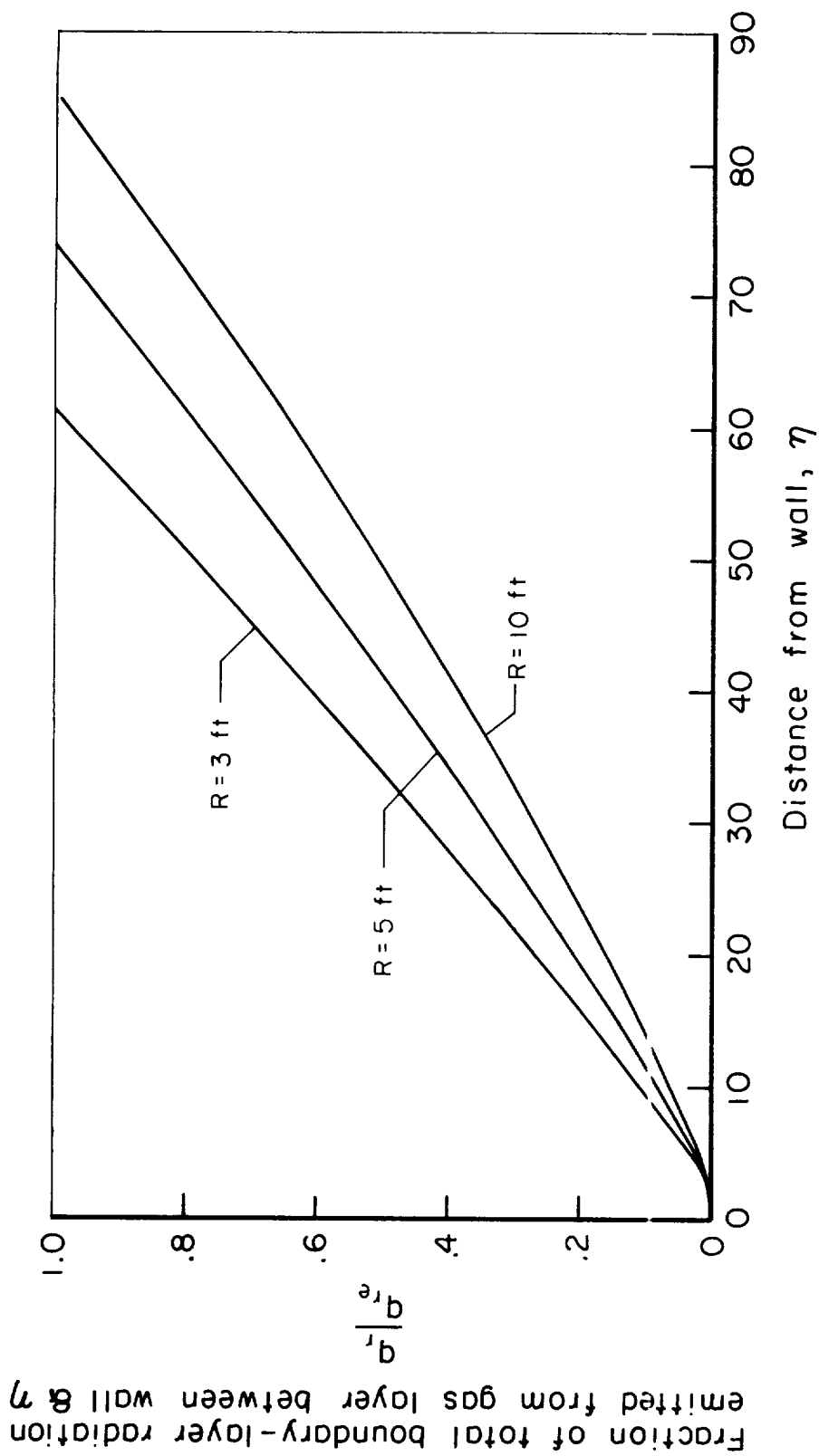


Figure 4.- Integrated radiant energy emission in boundary layer for various nose radii (31,000 ft/sec at 165,000 ft altitude, $T_w = 2000^\circ \text{K}$).

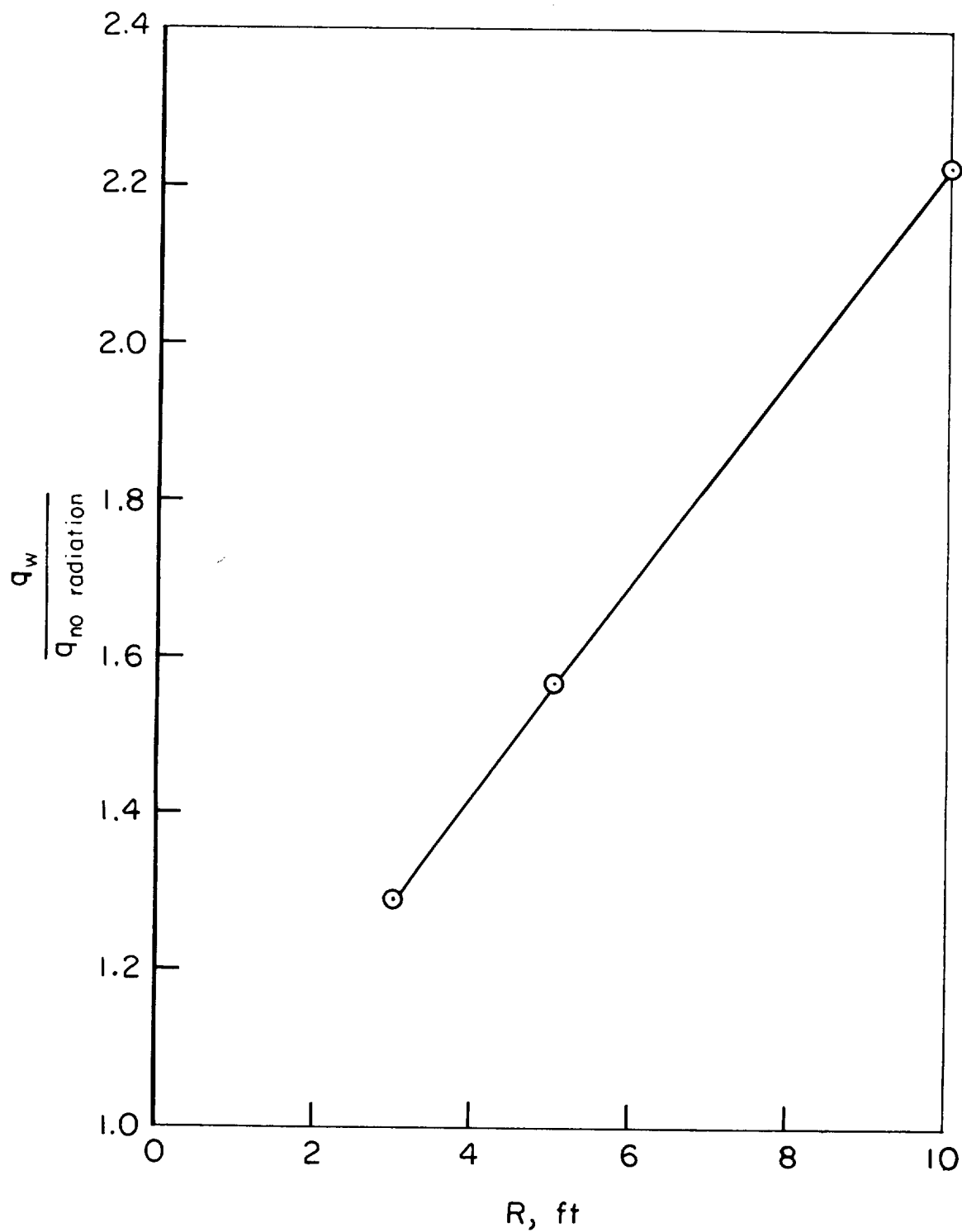


Figure 5.- Ratio of total boundary-layer heat transfer to wall with radiation to that without radiation as a function of nose radius (flight speed 31,000 ft/sec at 165,000 ft altitude, $T_w = 2000^\circ \text{ K}$).

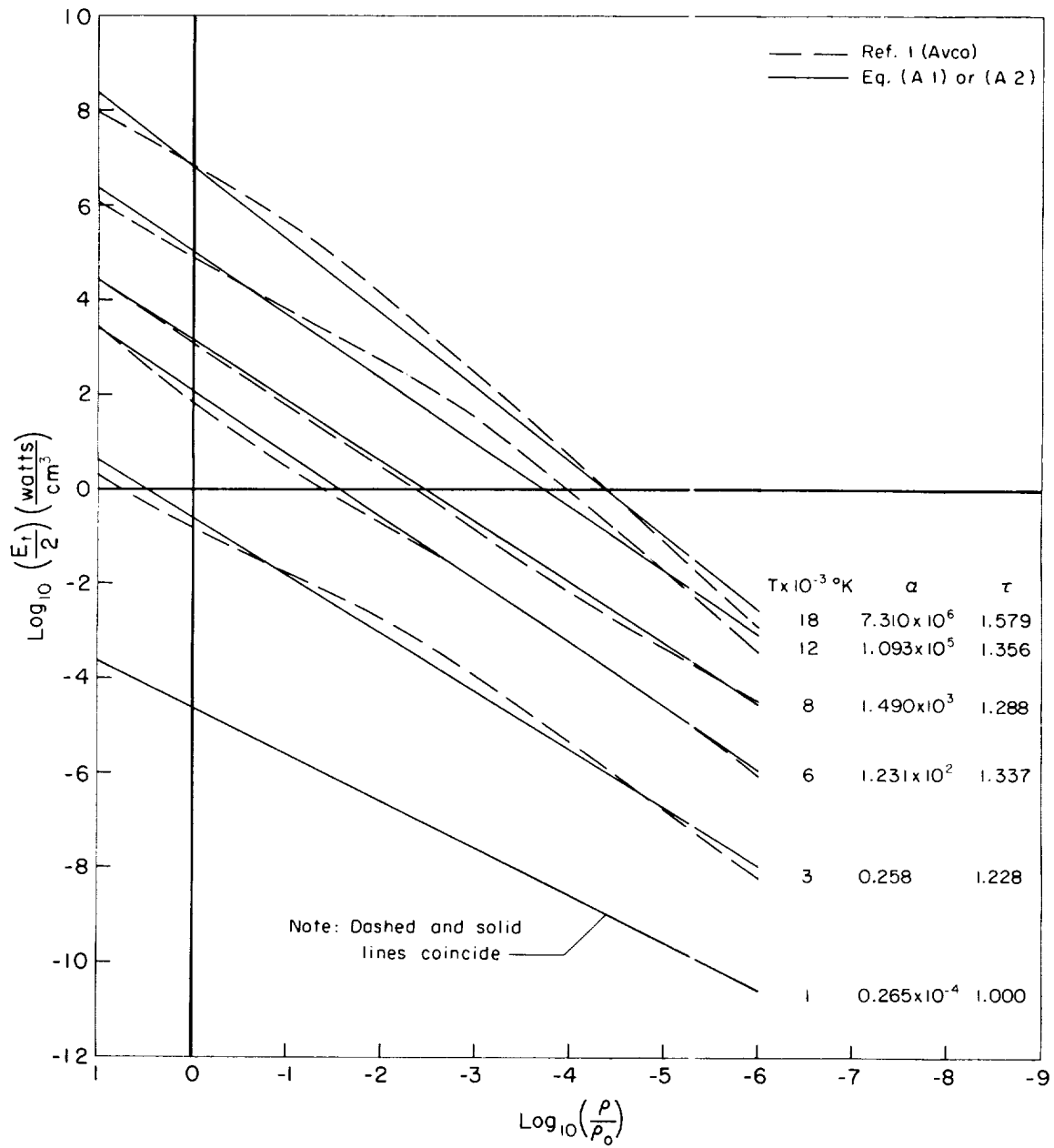


Figure 6.- Correlation for individual temperatures.

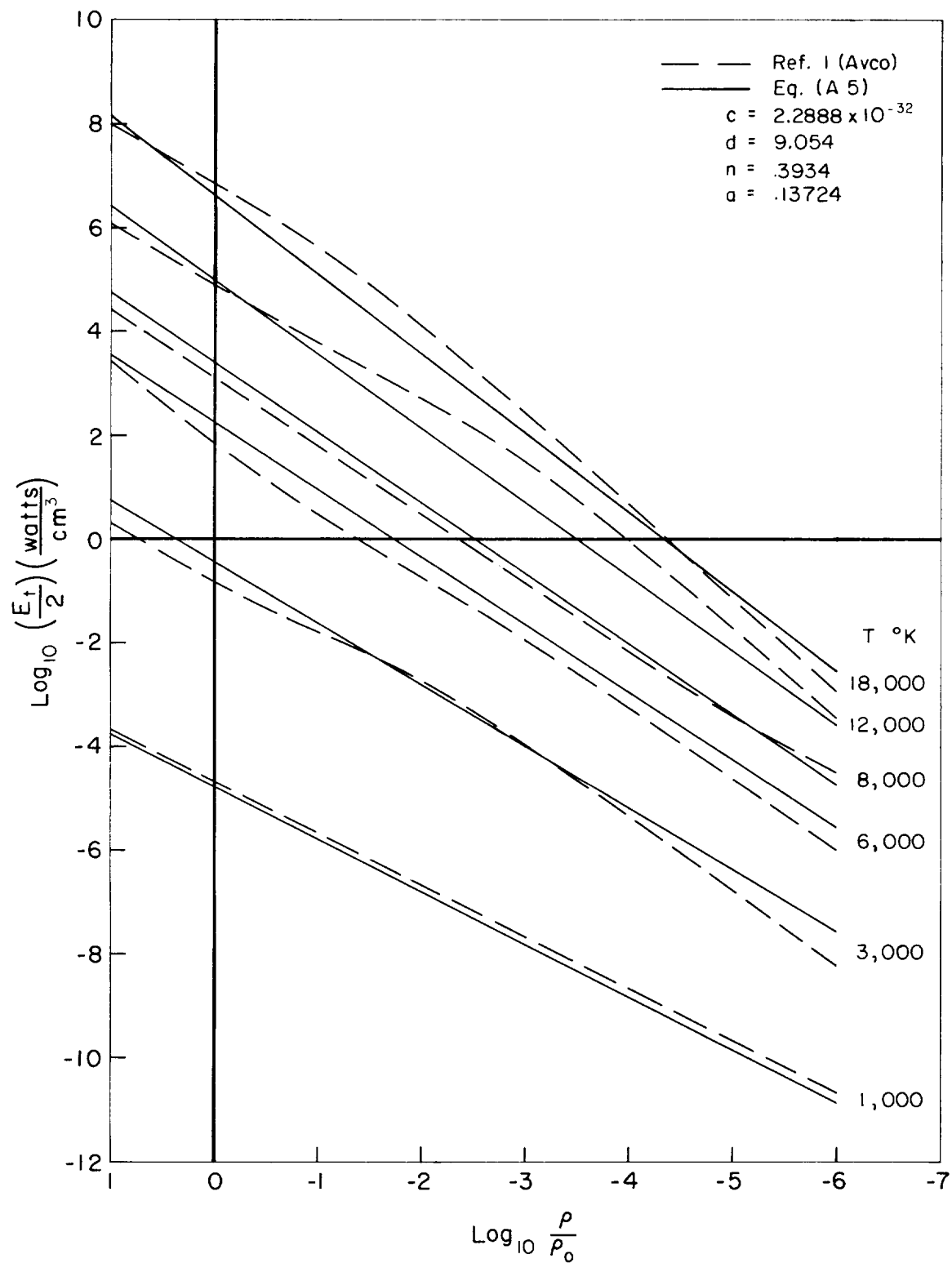


Figure 7.- General correlation of all data.

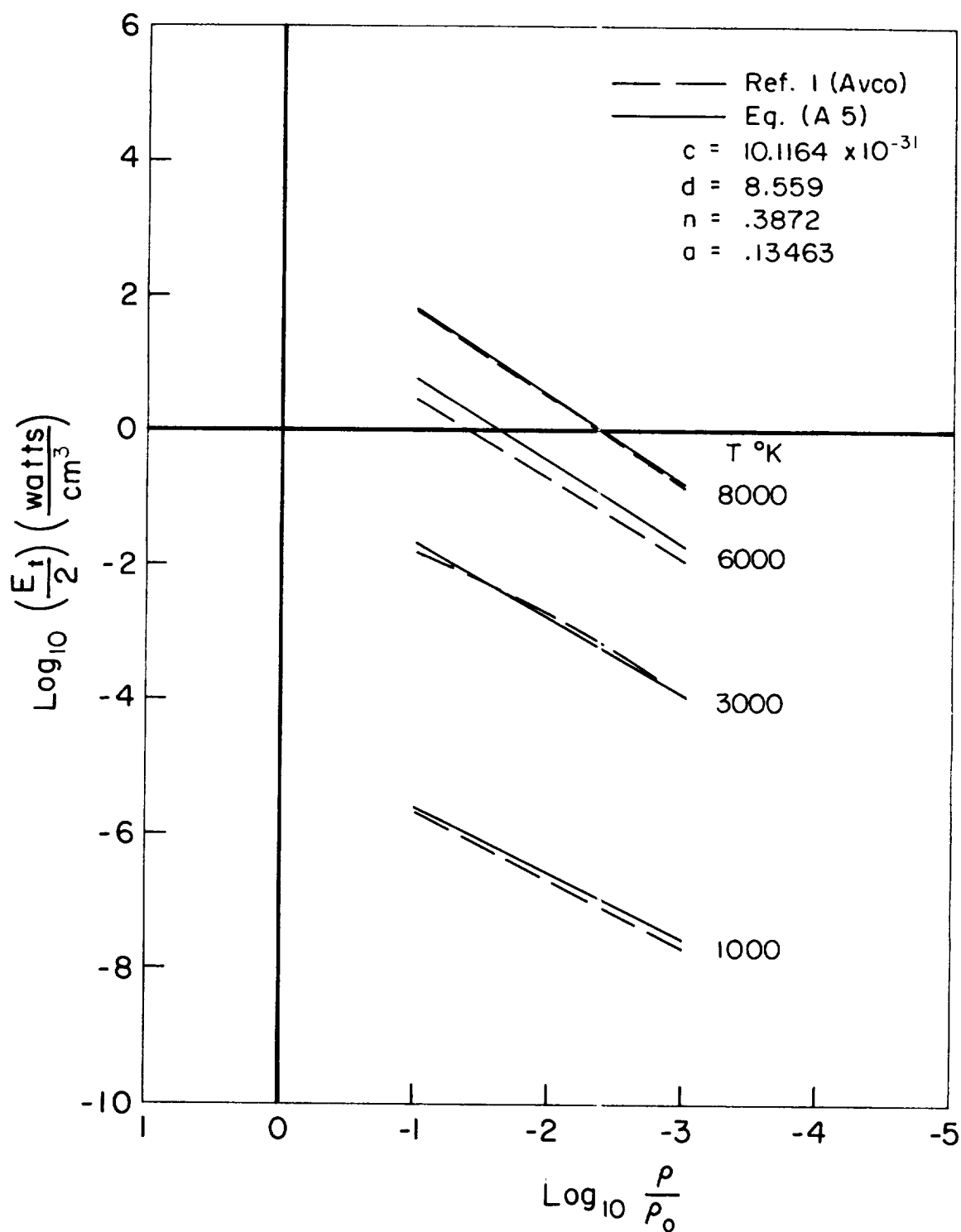


Figure 8.- Selected correlation of data (using 1000°, 3000°, 6000°, 8000° K data in density range $10^{-3} \leq \rho/\rho_0 \leq 10^{-1}$).

